Scientific Research and Essays Vol. 5(13), pp. 1615-1631, 4 July, 2010
Available online at http://www.academicjournals.org/SRE
ISSN 1992-2248 ©2010 Academic Journals

Full Length Research Paper

Seismic slope stability analysis: Gurpinar (Istanbul) as a case history

Ferhat Ozcep[1]*, Engin Erol[2], Fatih Saraçoğlu[3] and Mustafa Haliloğlu[4]

[1]Department of Geophysical Engineering, Faculty of Engineering, Istanbul University, Istanbul, Turkey.
[2]Granit Jeofizik, Catalca, Istanbul, Turkey.
[3]SRC Geoteknik ve Deprem Mühendisliği, Istanbul, Turkey.
[4]Jeoson Yeraltı Araştırma ve İnşaat Merkezi, Istanbul, Turkey.

Accepted 17 February, 2010

Slope failures triggered by the earthquakes are one of the most important soil problems. In this study, dynamic (earthquake) slope stability analysis was carried out in Gurpınar area. For this aim, in situ tests (SPT) were carried out and laboratory samples were obtained from 6 boreholes (their max. dept 50.0m) to determine soil classification and strength characteristics. Moreover, geophysical studies (seismic refraction and MASW) were also carried out in the area to estimate the structure and strength characteristics of the slope to 50.0 m. All of data, obtained in field and laboratory, was used to construct the mechanical and structural (geometrical) behavior of the slope. To solve slope stability problem, tree soil slope model was considered for the area. In dynamic state, to estimate the earthquake acceleration seismic hazard analysis was carried out in the region. In the end of the analysis, while there is not any problem in static condition/loads, some slope stability problems was appeared with increasing earthquake acceleration. A geotechnical slope improvement project was proposed for the study area.

Key words: Seismic slope stability, earthquakes, Gurpinar (Istanbul)

INTRODUCTION

Slope instability is responsible for damage to public and private property every year. Slope failures can be manifested as landslides or by more slowly processes such as soil creep. Buildings and infrastructure located on or in the path of a landslide can be seriously damaged or destroyed. Slope instability is a complex phenomenon that can occur at many scales and for many reasons. Slope stability analyses and stabilization require an understanding and evaluation of the processes that govern the behavior of slopes. Examples of triggering mechanisms or agitation factors of slopes include earthquakes, water, slope angle, slope strength characteristics.

The essential of geological, hydrological and seismological subjects related to the slope must be understood as well as the methods for obtaining the data necessary for input to reliable slope stability analyses. Scientists and engineers utilize many tools to investigate all aspects of slope instability. Key factors in the slope stability investigation include determining the boundaries of the slope instability, establishing a history of previous slope movement, assessing landslide causation, modeling landslide initiation as well as the travel paths taken by moving landslide debris, assessing the damage to affected buildings and structures, and preparing recommendations for stabilizing slopes.

First of all, slope failure is related to the following reasons:

(1) Soil properties or soil type of slope
(2) Geometry of slope
(3) Weight
(4) Water content (one of the most aggressive factors)
(5) Shearing strength reducing of slope
(6) Tension Cracks
(7) Vibrations and earthquakes

*Corresponding author. E-mail: ferozcep@istanbul.edu.tr.

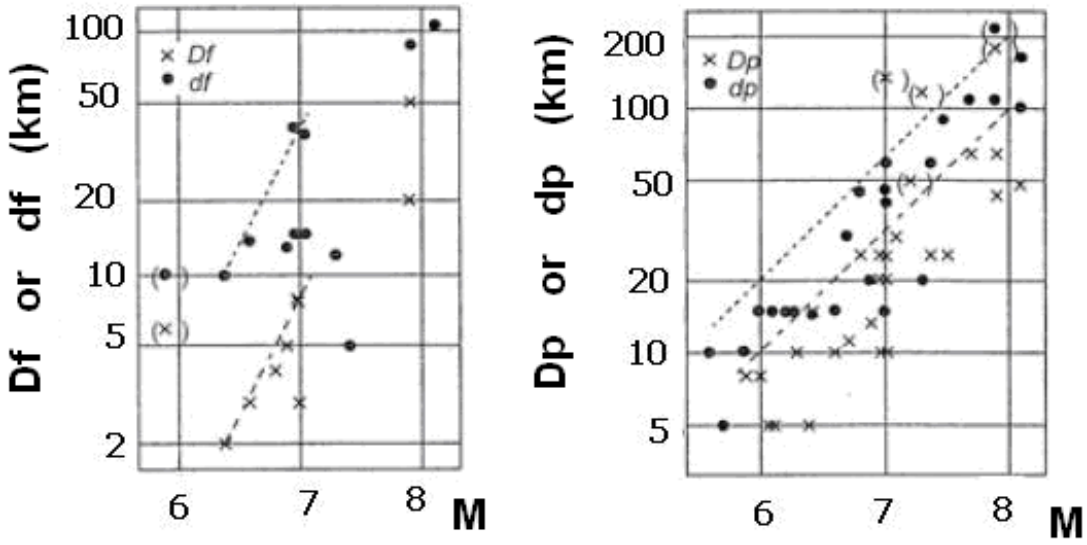

Figure 1. Relationship between magnitude and distance to slope failure in Japan (Tamura, 1978; ISSMFE, 1993).

The estimate of earthquake risk in city planning process is one of the most important duties in order to avoid natural disasters. The seismic risk evaluation includes the vulnerability of the value at risk and the hazard. Slope stability generated by seismic events will be invest-tigated. There are several studies about seismic slope stability analysis in literature (Matasivic, 1991; Bourdeau et al., 2004; Cherubini et al., 2004).

The main goal of this research that carried out in Gurpınar (Istanbul) as a case history is an evaluation of prevailing techniques for static and seismic slope analysis and mitigation of earthquake-induced landslides produced by seismically induced ground deformations.

Earthquakes and slope failures

Earthquakes and related slope failures for Japan were investigated (shown in Figure 1) by Tamura (1978). In this figure, Df is the distance from a fault to an outer boundary of the zone where many slope failures occurred; df is the distance from a foult to an outer boundary of the zone where few slope failures occurred; Dp is the distance from an epicenter to an outer boundary of the zone where many slope failures occur and dp is the distance from an epicenter to an outer boundary of the zone where few slope failures occurred.

In the “Manual for Zonation on Seismic Geotechnical Hazards” (prepared by the Technical Committee for Earthquake Geotechnical Engineering, TC4, of the Inter-national Society for Soil Mechanics and Geotechnical Engineering), the magnitude-distance criteria and historic information is summarized in Figure 2 and Figure 3.

Curves shown in Figure 4 are recommended for use in microzoning giving maximum epicentral distance for slope failure as a function of magnitude.

SLOPE STABILTY EVALUATION METHODS

Slope stability evaluation methods may be divided static and seismic slope stability methods.

Slices method (static load state) for effective soil pressure state

Safety factor (FS) for slope stability with undrained shear strength parameters (φ’ ve c’) could be given in the following equation:

$$FS = [\Sigma\, c'\, bi/\cos\alpha i + \tan\varphi' \,\Sigma\, Wi \cos\alpha i - ubi/\cos\alpha i\,]/\Sigma Wi \sin\alpha i) \quad (1)$$

Where u pore water pressure (u= hw.γw), and other parameters were given in Figure 5.

Slices method (seismic load state) for effective soil pressure

Parameters that used in seismic slope stability analysis were given in Figure 6. Forces acting on the failure surface are as follows:

(a) Weight of wedge, W;
(b) Inertia force on the wedge, k_hW, where k_h is the average coefficient of horizontal acceleration, and
(c) Resisting force per unit area, s, which is the shear strength of soil acting along failure surface, ABC. Safety factor with respect to strength, FS: is calculated as

FS = resisting moment about O /overturning moment about O = $S(ABC)R/WI_1 + K_hWI_2$

In the analysis for stability of slopes, it is assumed that soil is homogeneous. However, in a given slope, layered soil can be encountered. In order to explain this method, let us consider a

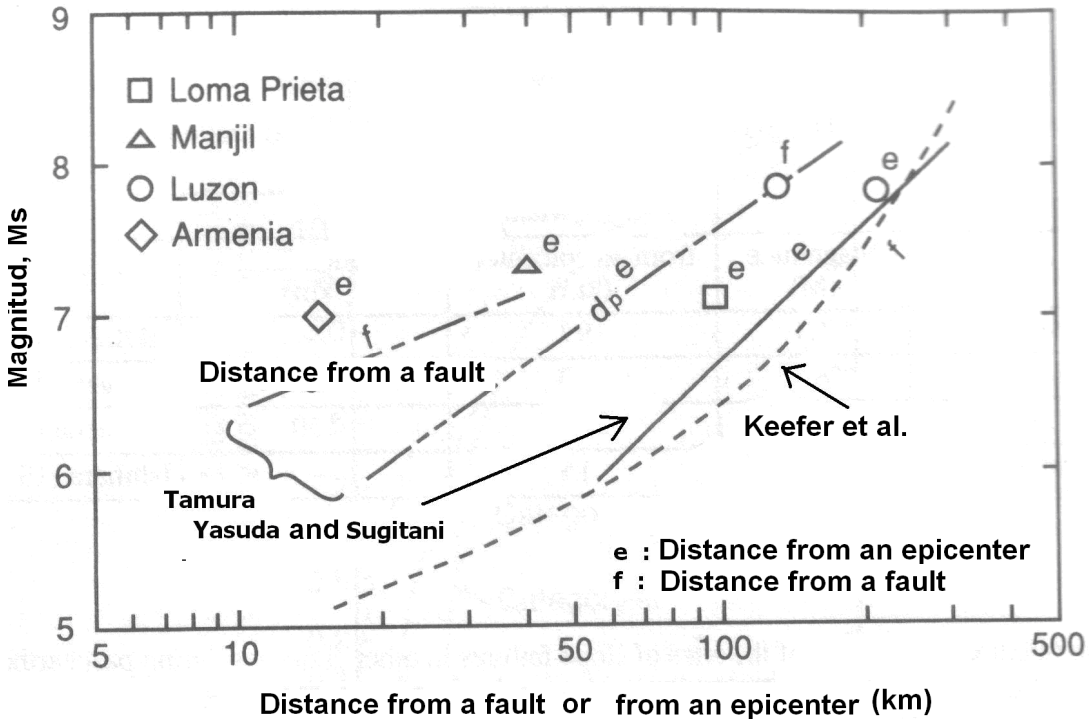

Figure 2. Comparison of relationships between magnitude and maximum distance from a fault or an epicenter (ISSMFE, 1993).

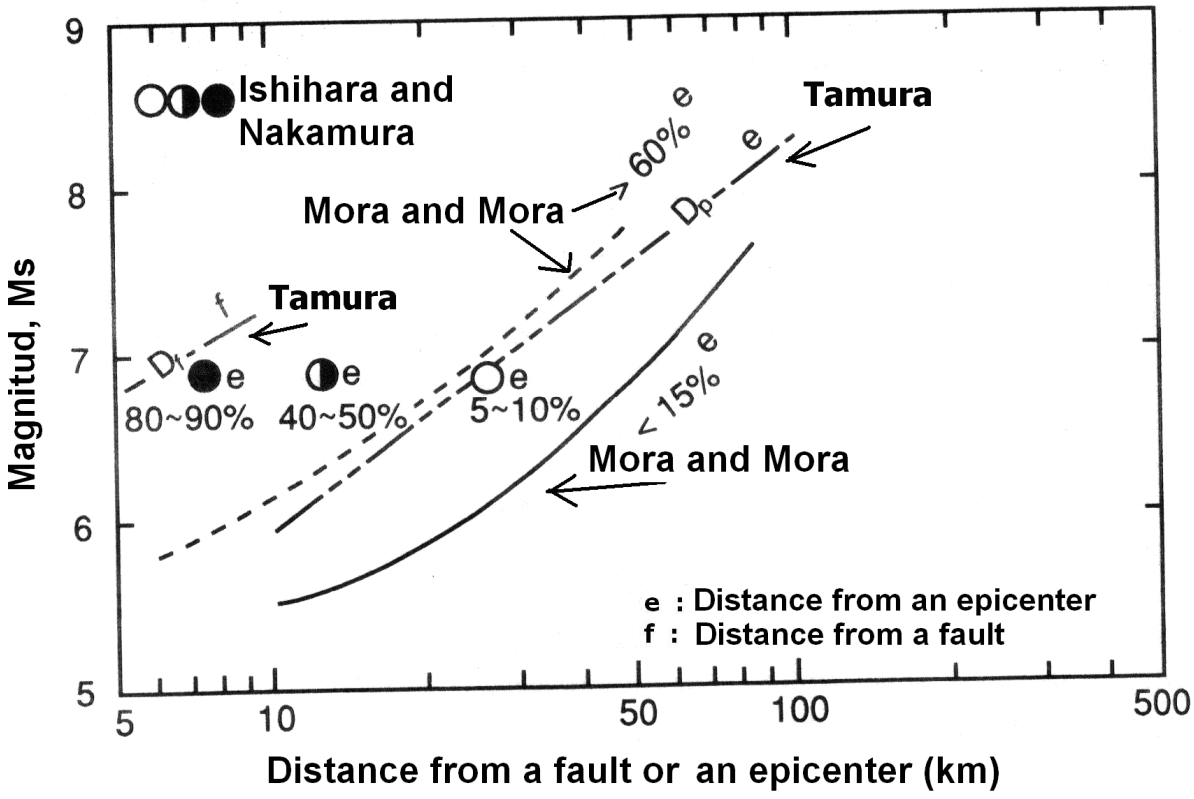

Figure 3. Comparison of relationships between magnitude and distance from a fault or an epicenter causing different percentage of slope failures (ISSMFE, 1993).

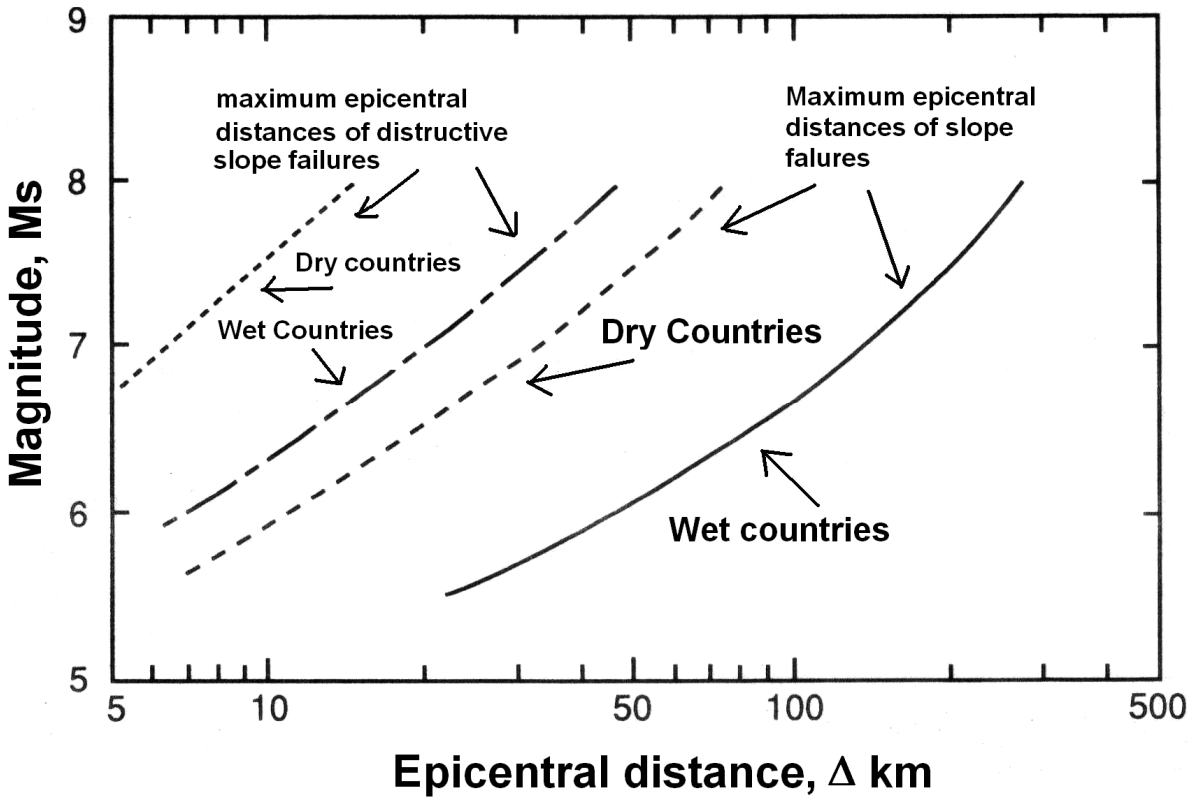

Figure 4. General Relationships between magnitude and the epicentral distance of slope failures.

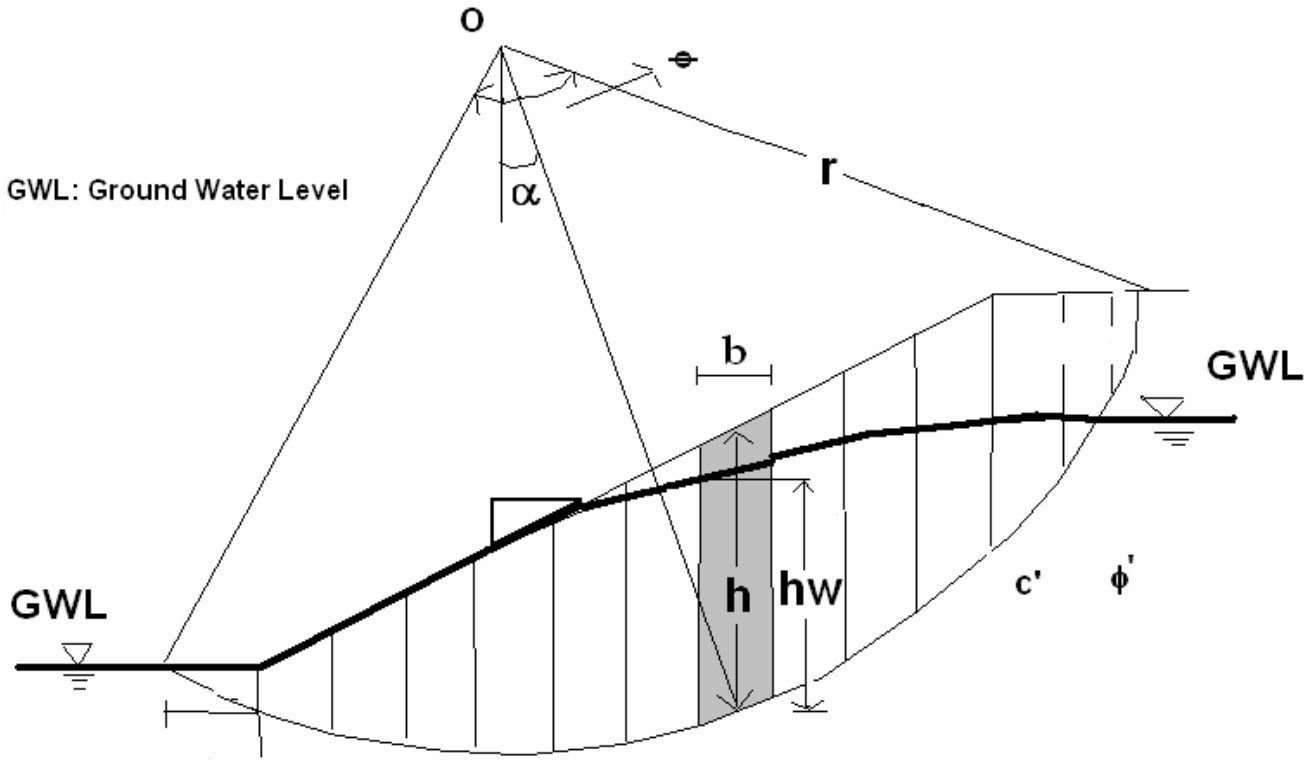

Figure 5. Slope parameters with undrained shearing strength parameters (φ' ve c').

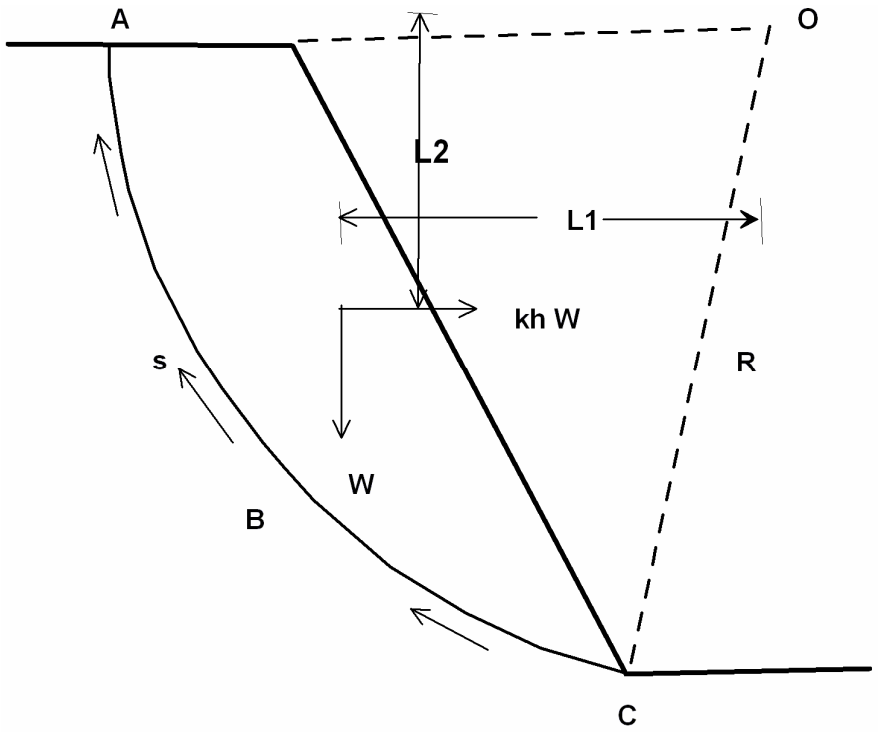

Figure 6. Parameters for seismic slope stability (Redrawn from Das, 1993)

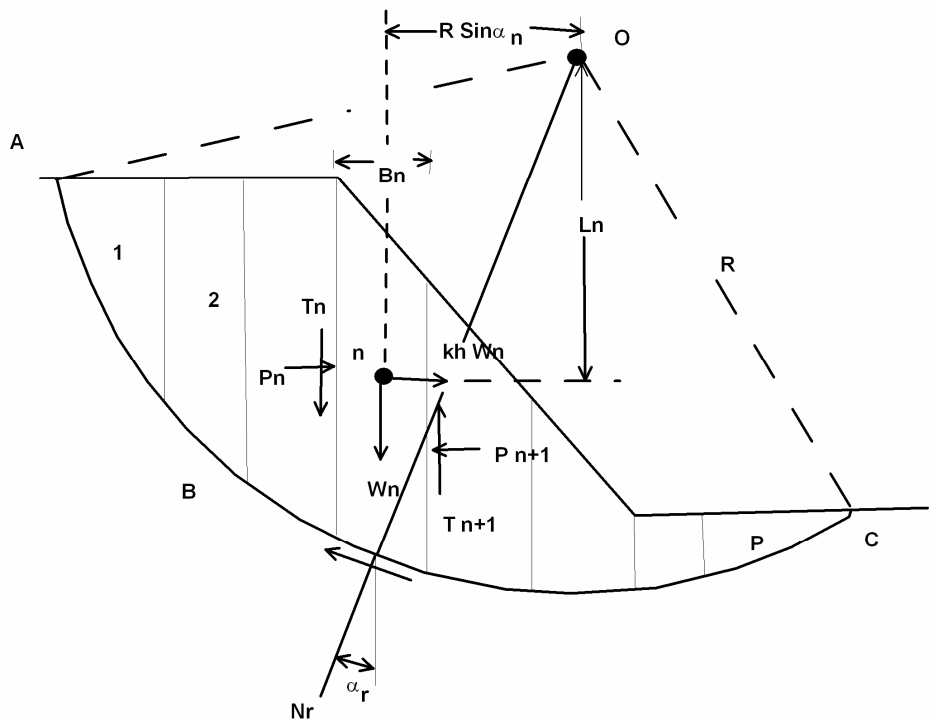

Figure 7. Parameters for Seismic Slope stability analysis (Redrawn from Das, 1993)

safety factor of this slope is given in the following equation (Das, 1993).

slope shown in Figure 7.

$$GK = [\Sigma^{p}_{n=1} (cB_n \sec\alpha_n + WnCos\alpha_n \tan\varphi)]/[\Sigma^{p}_{n=1} ([W_n Sin\alpha_n + kh$$

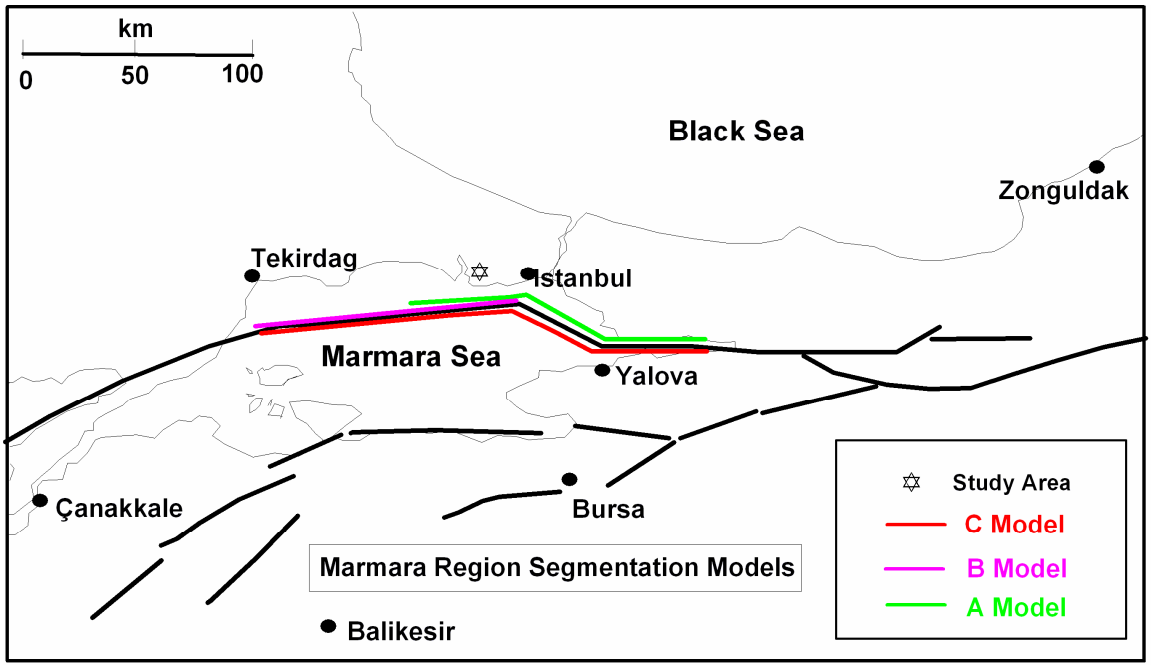

Figure 8a. For Marmara Region, it was assumed four model (A, B and C) for seismic hazard. Model A: approximately 119 km rapture length; Model B: approximately 108 km rapture length; Model C: approximately 174 km rapture length

W_n (Ln/R)]] (2)

where, αn may be either positive or negative.

ANALYSIS FOR STUDY AREA

Study area and general geology

Study area was shown in Figure 8a. General geology of area is formed by Trace formation, Gurpinar formation, Kirklareli formation, Sazlıdere formation, Bakırköy formation and çukurçeşme formation (Alpaslan, 2006). Gurpinar formation is Miocene and upper Oligocene aged and it includes sandstone, milestone, claystone units, and several soil components mainly clays.

Geophysical and geotechnical (borehole) studies

In the early 1980s, a wave-propagation method to generate the near-surface *vs* profile, called spectral analysis of surface waves (SASW), was introduced (Nazarian et al., 1984). SASW uses the spectral analysis of ground roll generated by an impulsive source and recorded by a pair of receivers. This method has been widely and effectively used in many geotechnical engineering projects (Stokoe et al., 1994). The necessity of recording repeated shots into multiple field deployments for a given site increases the time and labor requirements over a multichannel procedure. Multichannel analysis of surface waves (MASW) tries to overcome the few weaknesses of the SASW method (Park et al., 1999). The multichannel analysis of surface waves (MASW) method deals with surface waves in the lower frequencies (e.g., 1 – 30 Hz) and uses a much shallower depth range of investigation (e.g., a few to a few tens of meters) (Park et al., 2007).

The shear wave velocities and profile are obtained by multi channel analysis of surface wave in study area. The phase velocity-dispersion curve and shear wave velocity are obtained by inversion distance profile for first 50 meters of soil. An example application for slope site is shown in Figure 8b in which are shown the data records. The records that are depending on field conditions with different geophone intervals are taken.

Passive source when it is compared by active source reaches deeper parts of soils, because the lower frequency of natural noises are recorded different noises that are given more information from the deeply distance. In our study the linear arrays are applied.

After the data are collected from the field, data-processing are carried out, the phase velocities for the different frequency are obtained by using Pickwin program and the end of the process, dispersion curve is obtained (Figure 8c).

During the field studies, the seismic refraction data are also collected. The initial model that obtained from these data is used the initial model data. By using both forward and inverse solutions algorithm, S wave velocities are calculated and drown depending on distance (Figures 8d and e).

In this study, Geometrics Smart Seis SE seismic instrument, geophone and other seismic tools are used. The records that obtained from measurement are controlled in the field, after made necessary arrangement obtained the refraction measurement and dynamic and elastic parameters are modeled and explained by using computer program the named Seis Imager 1D Pickwin / Surface Wave Analysis.

Finally, cross-section (obtained from Vp velocities) is given in Figure 8f. In this Figure, slope structure for fist 19.0 m is given with V p and Vs velocities. In the study area, borehole study was also carried out at 9 points from 15 up to 50 m. One example of these boreholes was given in Figure 8g, 8h, and 8i.

Seismic hazard analysis of study area

Seismic hazard analysis is the computation of probabilities of occurrence per unite time of certain levels of ground shaking caused by earthquakes (Erdik et al., 1999, 2004). This analysis is

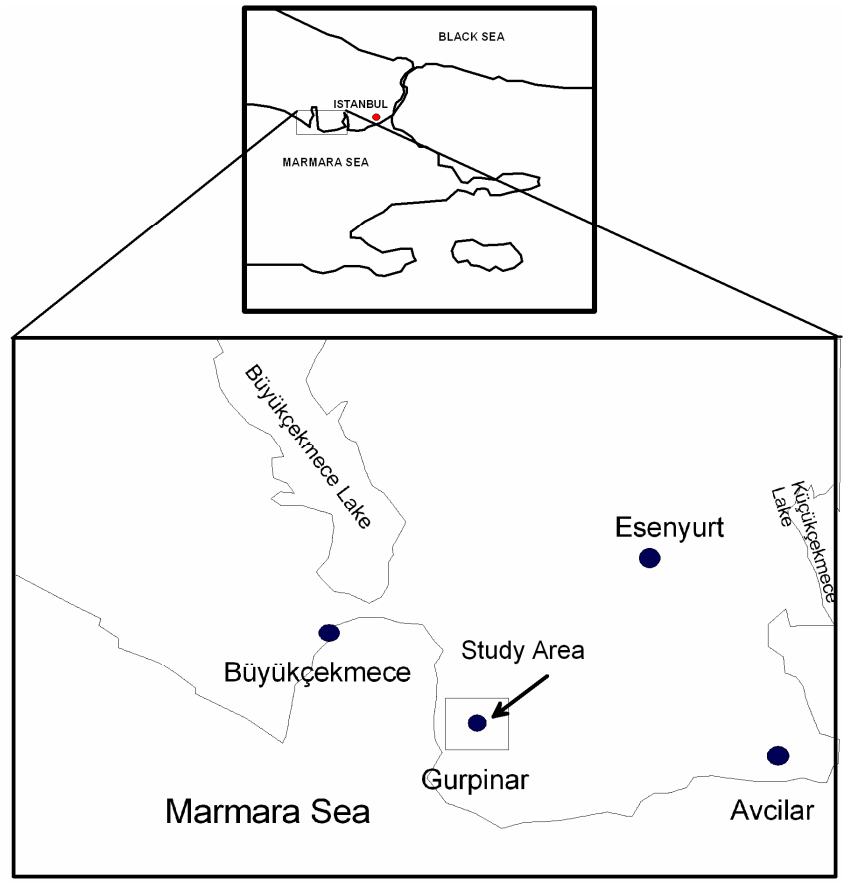

Figure 8b. Study area.

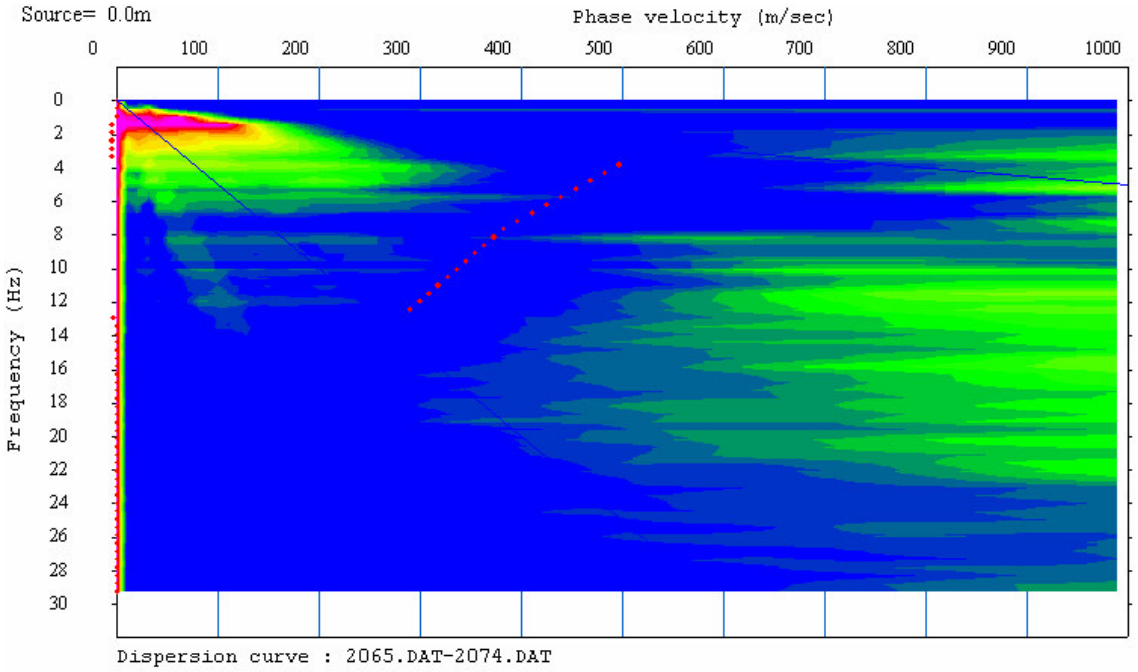

Figure 8c. The formation of the dispersion curve (for site 36). Phase velocities and frequencies are determined time-spatial surface–wave data with two dimensional Fourier analysis.

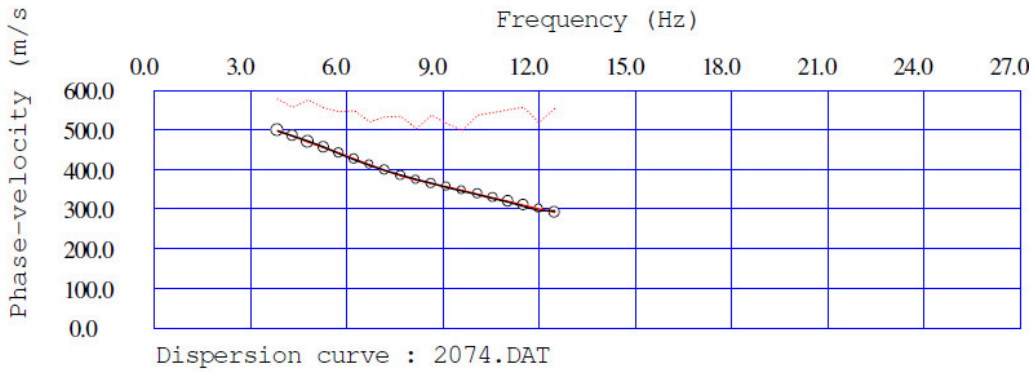

Figure 8d. Phase velocity – frequency curve (for slope).

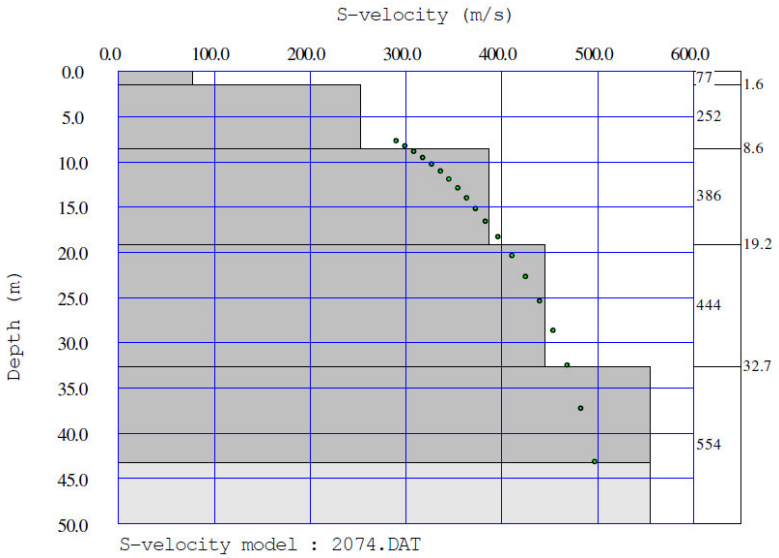

Figure 8e. S velocity – depth section.

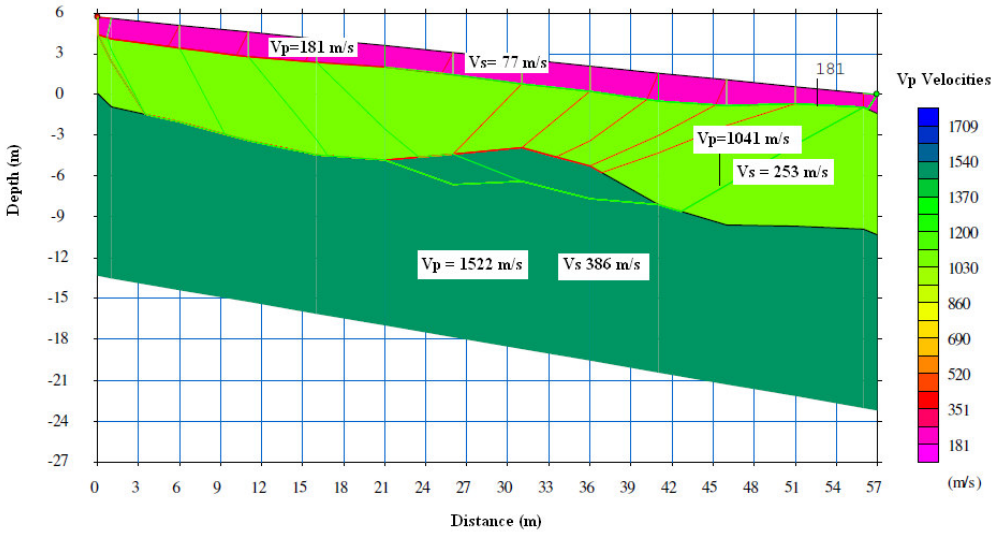

Figure 8f. Geophysical cross-section (obtained from Vp velocities) of study area.

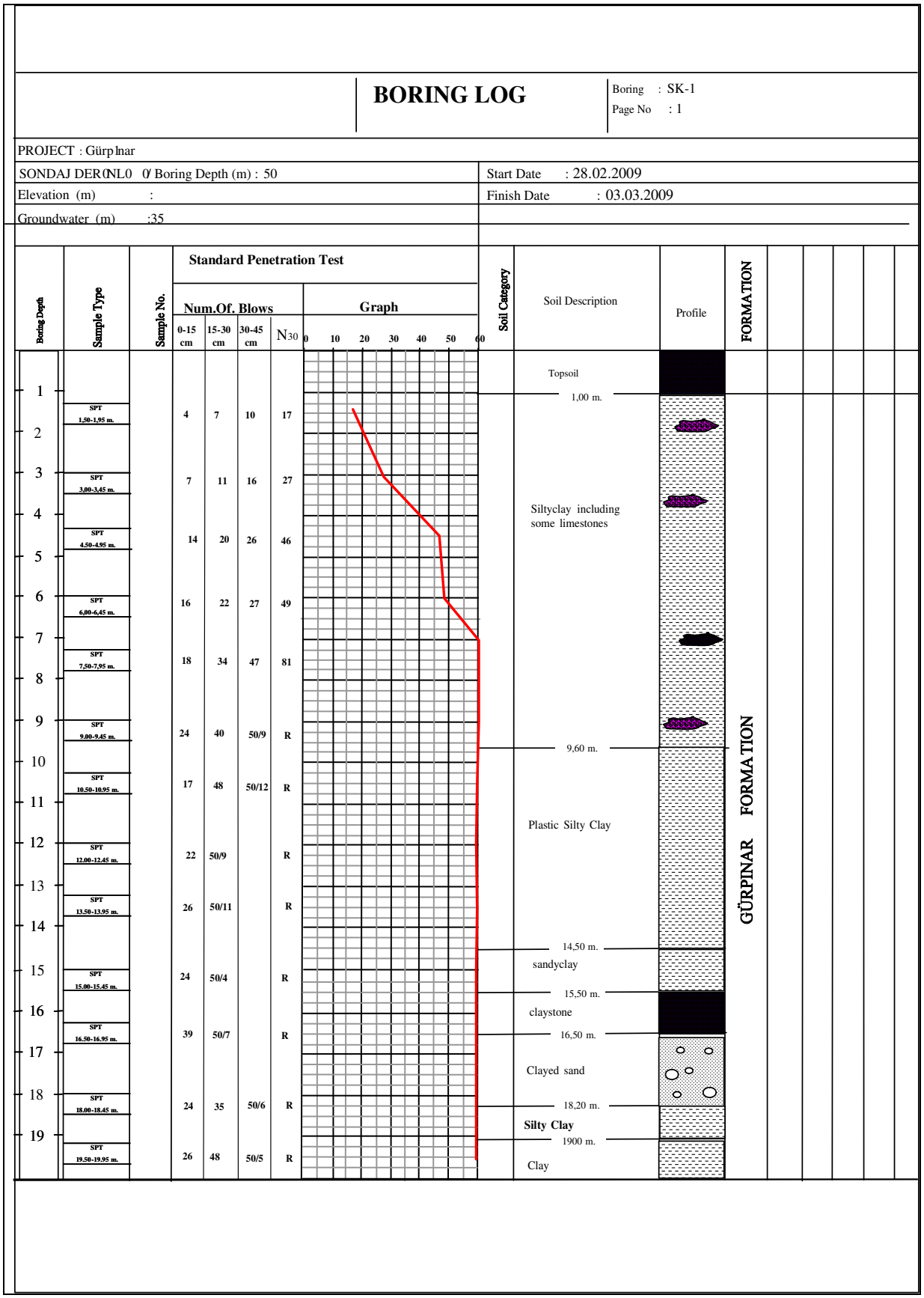

Figure 8g. Borehole log in project area, for first 20 m of depth.

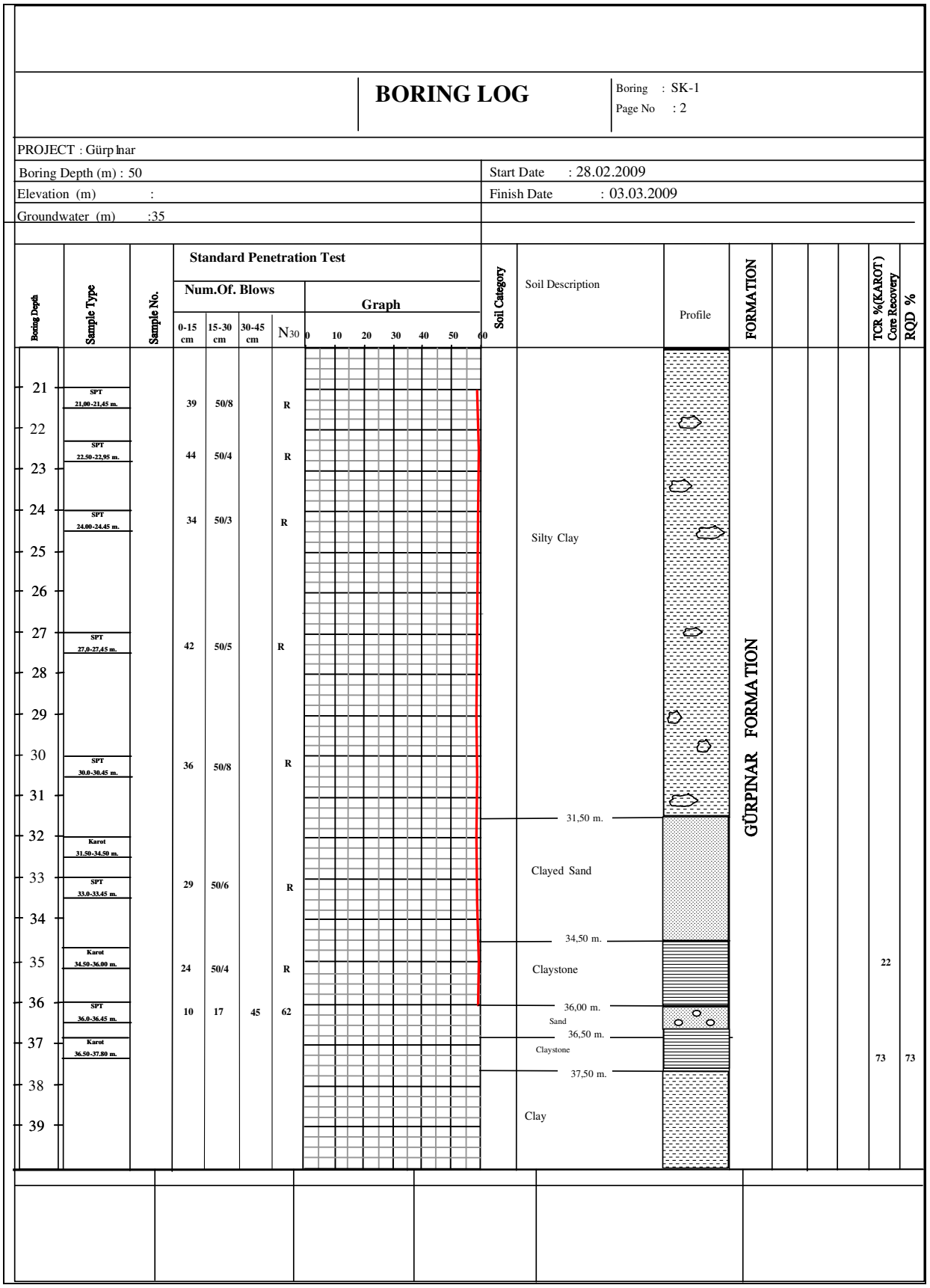

Figure 8h. Borehole log in project area for depths between 21 - 40 m.

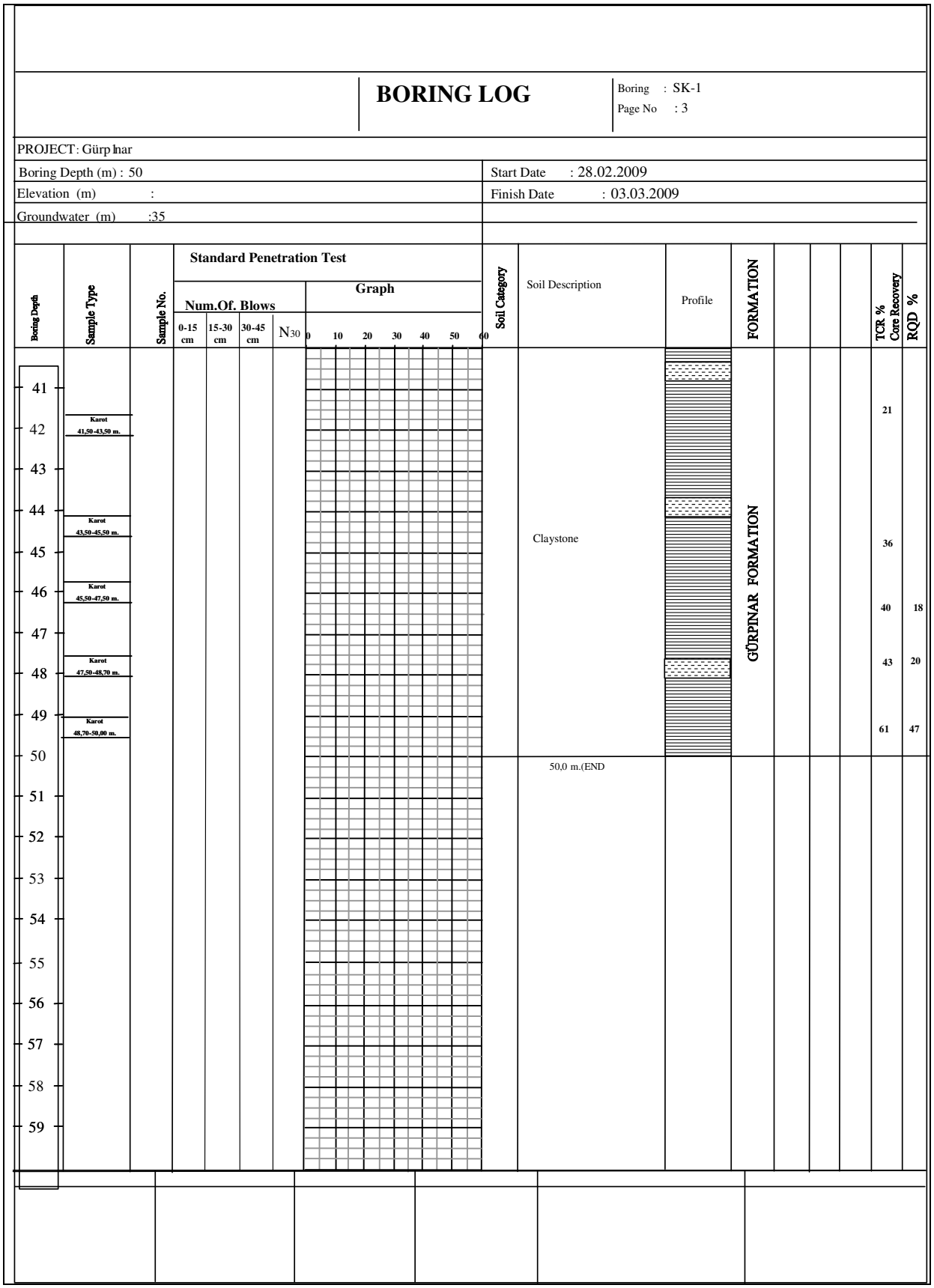

Figure 8i. Borehole log in project area for depths between 41 - 50 m.

Table 1a. Equations for rapture length and magnitude estimations.

Researcher	M (magnitude)	Magnitude type
Abraseys and Zatopek (1968)	M = (0.881 LOG(L))+5.62	Ms
Douglas and Ryall (1975)	M = (LOG(L)+4,673)/0.9	Ms
Ezen (1981)	M = (LOG(L)+2,19)/0.577	Ms
Matsuda (1975)	M = (LOG(L)+2,9)/0.6	Ms
Patwardan et al. (1975)	M = (LOG(L) 1,1)+5.13	Ms
Toksöz et al (1979)	M = (LOG(L)+3,62)/0.78	Ms
Wells and Coppersmith (1994)	M = 5.16 + (1,12 LOG(L))	Mw
Wells and Coppersmith (1994)	M = 5.08 + (1,16 LOG(L))	Mw

Table 1b. Model A: approximately 120 km rapture length; Model B: approximately 108 km rapture length; Model C: approximately 174 km rapture length. For these models, Rapture length and magnitude estimations.

Researcher	M (magnitude) ranges for A model	M (magnitude) ranges For B model	M (magnitude) ranges for C model
Abraseys and Zatopek (1968)	7.4	7.4	7.6
Douglas and Ryall (1975)	7.5	7.5	7.7
Ezen (1981)	7.4	7.3	7.7
Toksöz et al. (1979)	7.3	7.2	75
Wells and Coppersmith (1994)	7.5	7.4	7.7

Table 1c. Earthquakes in our area about 100 km radius.

Magnitude ranges	4.5 ≤ M < 5.0	5.0 ≤ M < 5.5	5.5 ≤ M <6.0	6.0 ≤ M <6.5	7.0 ≤ M <7.5
Numbers	31	12	7	1	1

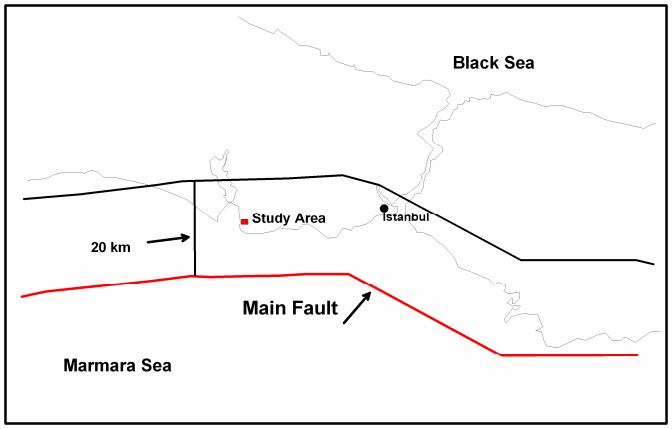

Figure 9. Sismogenetic fault for the study area.

often summarized with a seismic hazard curve, which shows annual probability of exceedence versus ground motion amplitude. Deterministic and Probabilistic seismic hazard analysis was used to evaluate the seismic hazard of Region. Potential earthquake source area was considered the North Anatolian Fault in Marmara Sea.

Deterministic seismic hazard analysis

Required input for deterministic hazard analysis is a designation of active faults or earthquake sources in the region. For Marmara Region (Figure 8), it was assumed four model (A, B and C) for seismic hazard (JICA-IBB Report, 2002). Model A: approximately 119 km rapture length. Figure 9 shows sismogenetic fault for the study area. Model B: approximately 108 km rapture length; Model C: approximately 174 km rapture length. For these models, magnitudes were estimated (Tables 1a and b).

Probabilistic seismic hazard analysis of region

In Table 1c, earthquakes were given in our area about 100 km radius. Gutenberg-Richter recurrence relationships was determined as

$$\text{Log}(N) = 3.0 - 0.71\,M \quad (1)$$

Earthquake occurrence probability were given in Table 2a by using $Rm = 1 - e^{-(N(M)\cdot D)}$

Where Rm = Risk value (%); D, duration; N(M) for M magnitude (1) equation value.

Attenuation relationship was defined by two attenuation model. From a set of attenuation relationships, the design acceleration values of the city was calculated as 0.41 g (for Joyner and Boore (1981) model) and 0.4 g (Campbell (1997) model) with exceeding

Table 2a. Earthquake occurrence probability for region.

Magnitude	For D = 10 (Years) probability (%)	For D = 50 (Years) probability (%)	For D = 75 (Years) probability (%)	For D = 100 (Years) probability (%)
5	92.4	100.0	100.0	100.0
5.5	67.7	99.6	100.0	100.0
6	39.0	91.6	97.5	99.3
6.5	19.4	66.1	80.3	88.5
7	9.0	37.7	50.8	61.2
7.6	4.1	18.7	26.7	33.9

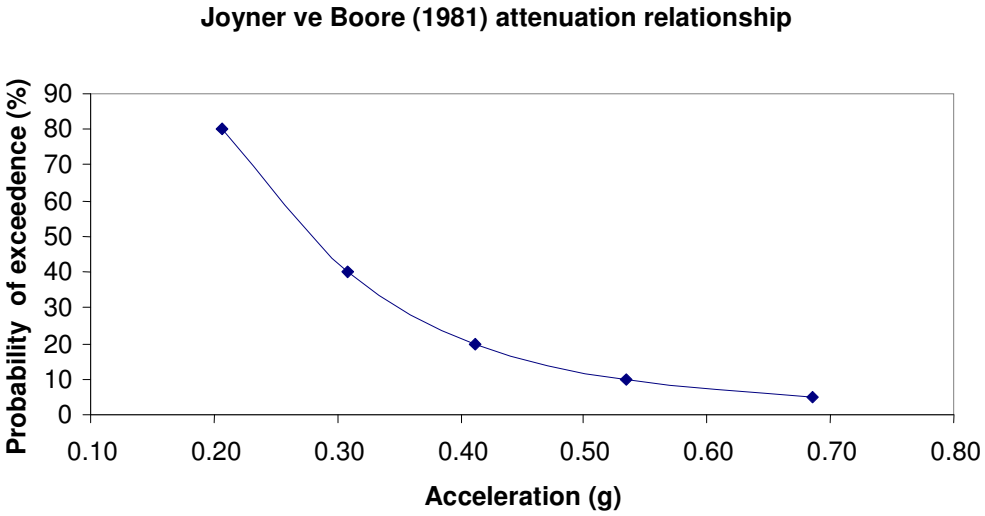

Figure 10. Hazard Curve for region by using Joyner and Bore (1981) attenuation model.

probability of 20 % in 50 years. Finally, hazard curve for region was estimated (in Figure 10). Estimated acceleration values for 7.5 magnitude was given in Table 2b.

Design acceleration coefficient, kh was selected by following equations:

kh= (0.3(I+1)Ao)

and

kh=(0.2(I +1) Ao)

where; I= Structure Importance factor (its value is varied from 1 to 1.5), Ao = estimated earthquake acceleration (0.43 g).

In this study, kh coefficient was selected as 0.20 g. If it is examined earthquake and slope triggering relation as shown in Figures 1, 2 and 3, with study area of 15 km epicentral distance to main fault, minimum 6.0 magnitudes may trigger the slope on the study area. For this reason, detailed seismic slope stability analysis was carried our fort he study area.

Detailed slope stability analysis for static and seismic conditions

In the study area, in situ tests (SPT) were carried out and laboratory samples were obtained from 6 boreholes (their max. dept 50.0 m) to determine soil classification and strength characteristics. Moreover, geophysical studies (seismic refraction and MASW) were also carried out in the area to estimate the structure and strength characteristics of the slope to 50.0 m. All of data, obtained in field and laboratory, was used to construct the mechanical and structural (geometrical) behavior of the slope. To solve slope stability problem, tree soil slope model was considered for the area.

Geometric features and the failure surface of the first, second and third model was shown in Figures 11a, b and c. Results for analysis was given in Tables 3a, 3b, 3c and 3d.

RESULTS AND DISSCUSSION

Matasivic (1991) point out, seismic stability of natural slopes is a subject about which much uncertainly still exist. Main problems associated with predicting slope behavior during and after earthquake shaking are connected with selection of shear strength parameters of material and estimation of adequate seismic loading. In the other side, both the local topography and the presence of surface layers are likely to have caused the observed amplification effects, which are supposed to have contributed to the triggering of some of the hundreds of landslides related to this seismic event (Bourdeau et al., 2004). The stability of a slope during or

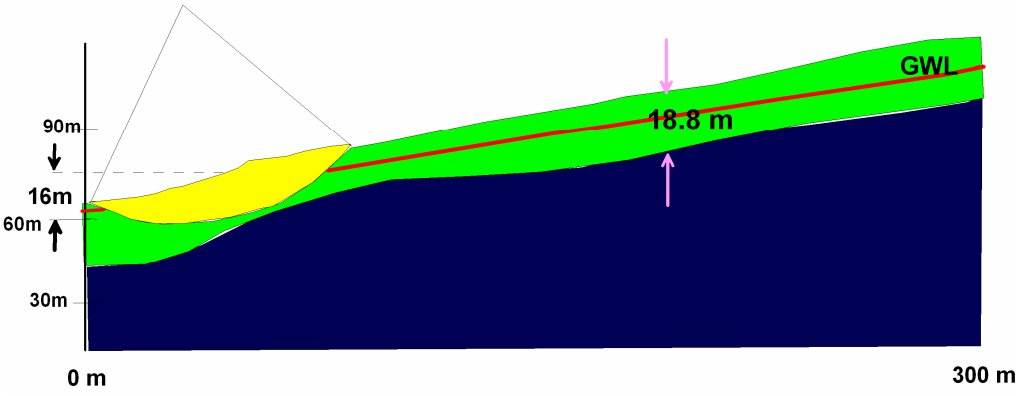

Figure 11a. First model.

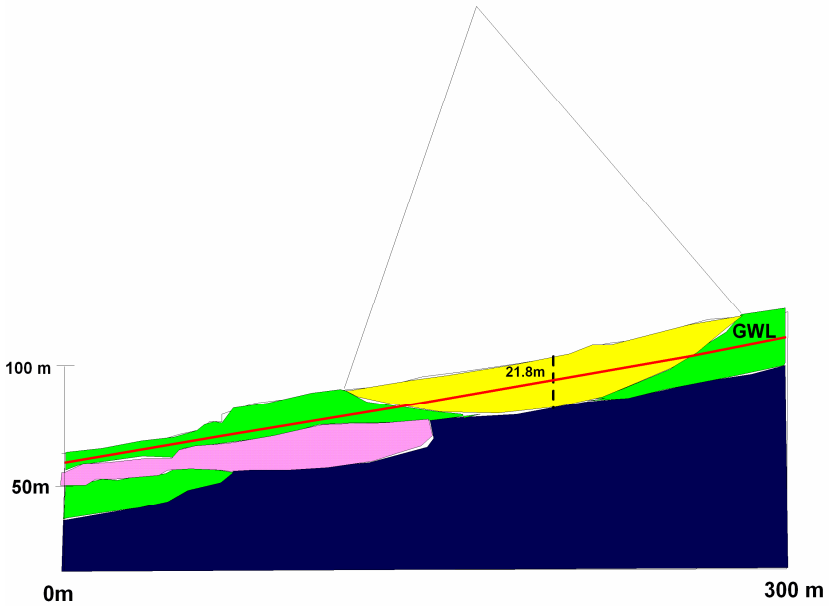

Figure 11b. Second model

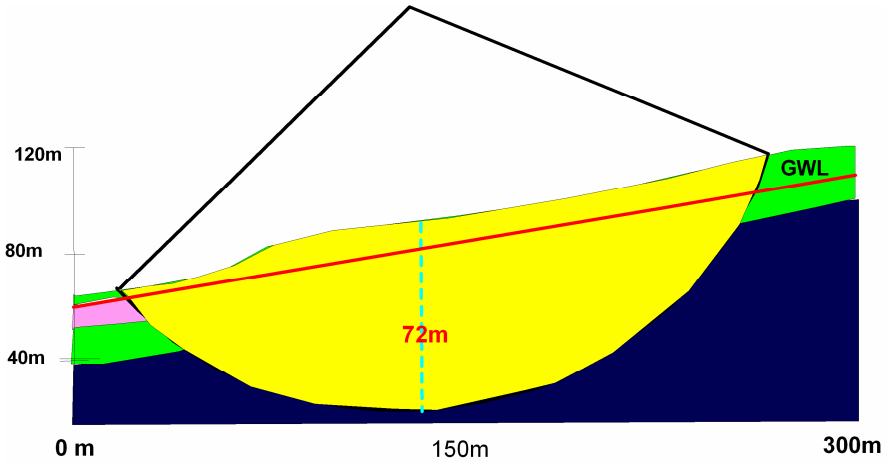

Figure 11c. Third model.

Table 3a. Safety factor for static and dynamic conditions with geometric and mechanical parameters for first slope model for R = 0 73.70 m

SF static	2.5
SF earthquake (for kh: 0.2)	1.2

Slice No	b (m)	h (m)	hw (m)	γ (kN/m^3)	α	c' (kPa)	ϕ'
1	7.1	3.3	0.1	19	-25.0	23	14
2	7.1	6.6	3.3	19	-20.0	23	14
3	7.1	7.9	4.6	19	-15.0	23	14
4	7.1	10.6	6.6	19	-10.0	23	14
5	7.1	13.2	7.3	19	-3.0	23	14
6	7.1	14.5	7.3	19	3.0	23	14
7	7.1	16.6	8.6	19	10.0	23	14
8	7.1	17.2	11.9	19	15.0	23	14
9	7.1	16.5	9.9	19	20.0	23	14
10	7.1	13.2	7.9	19	28.0	23	14
11	7.1	11.9	4.6	19	33.0	23	14
12	7.1	8.6	3.3	19	38.0	23	14
13	7.1	6.6	0.0	19	45.0	23	14

Table 3b. Safety factor for static and dynamic conditions with geometric and mechanical parameters for second slope model for R = 169.40 m.

SF static	1.5
SF earthquake (for kh: 0.2)	0.9

Slice No	b (m)	h (m)	hw (m)	γ (kN/m^3)	α	c '	ϕ'
1	13.7	3.8	0.0	19	-17.0	23	14
2	13.7	10.2	0.0	19	-13.0	23	14
3	13.7	14.8	3.8	19	-8.0	23	14
4	13.7	16.6	6.4	19	-5.0	23	14
5	13.7	19.2	6.4	19	1.0	23	14
6	13.7	19.2	6.4	19	6.0	23	14
7	13.7	21.8	7.6	19	10.0	23	14
8	13.7	19.2	7.6	19	15.0	23	14
9	13.7	17.9	7.6	19	20.0	23	14
10	13.7	14.0	5.1	19	25.0	23	14
11	13.7	12.8	1.6	19	28.0	23	14
12	13.7	10.2	0.0	19	35.0	23	14
13	6.9	3.8	0.0	19	39.0	23	14

after a seismic event was studied by means of by pseudo-static approach which estimates the stability of a slope under dynamic loads by the dynamic safety factor. As Cherubini et al. (2004) point out; this approach is not able to account for either the seismic displacements of the slope or the influence of the duration and the time variation of the seismic struck acceleration over the slope displacements.

In the first phase of the study, to determine the ground motion level that triggered the slope, seismic hazard analysis of region was carried out by deterministic and probabilistic means. Moreover, relationships between magnitude and distance from a fault or an epicenter causing slope failures were examined in context of the study area. Main seismogenetic source of the region is north anatolian fault zone in marmara sea.

Both static and seismic slope stability analysis was carried out and obtained safety factor of slope. While there is no problem for stability in static case, seismic safety factors are obtained as 0.8 and 0.9 that are unsafe

Table 3c. Safety factor for static and dynamic conditions with geometric and mechanical parameters for third slope model for R = 151.98 m, with assumptions of clayed soil.

SPT(N)	40

	Hara et al. (1971)	Stroud (1974) Minimum value	Stroud (1974) Average Value	Stroud (1974) Maximum value
Cohesion cu kPa	413	140	175	260
SF static	2.5			
SF earthquake (for kh: 0.2)	1.2			

Slice No	b (m)	h (m)	hw (m)	γ (kN/m^3)	α	c'	ϕ'
1	24.2	18.3	12.2	18	-37.0	175	14
2	24.2	34.2	30.5	18	-28.0	175	14
3	24.2	57.3	45.1	18	-18.0	175	14
4	24.2	67.0	56.1	18	-8.0	175	14
5	24.2	70.7	59.7	18	1.0	175	14
6	24.2	73.2	68.3	18	7.0	175	14
7	24.2	70.7	58.6	18	18.0	175	14
8	24.2	62.2	52.5	18	28.0	175	14
9	24.2	56.1	39.0	18	40.0	175	14
10	24.2	31.7	18.3	18	53.0	175	14
11	6.1	7.3	0.0	18	63.0	175	14

Table 3d. Safety factor for static and dynamic conditions with geometric and mechanical parameters for third slope model for R = 151.98 m, with assumptions of sandy soil.

SF static	2.5
SF earthquake (for kh: 0.2)	1.2

Slice No	b (m)	h (m)	hw (m)	γ (kN/m^3)	α	ϕ'
1	24.2	18.3	12.2	18	-37.0	38
2	24.2	34.2	30.5	18	-28.0	38
3	24.2	57.3	45.1	18	-18.0	38
4	24.2	67.0	56.1	18	-8.0	38
5	24.2	70.7	59.7	18	1.0	38
6	24.2	73.2	68.3	18	7.0	38
7	24.2	70.7	58.6	18	18.0	38
8	24.2	62.2	52.5	18	28.0	38
9	24.2	56.1	39.0	18	40.0	38
10	24.2	31.7	18.3	18	53.0	38
11	6.1	7.3	0.0	18	63.0	38

to stability. Slope improvement is proposed for the study area.

ACKNOWLEDMENT

We are grateful to geophysical engineer Kerim Avci from “Geometrik Mühendislik” Company to helping and to taking the MASW measurements.

REFERENCES

Bourdeau C, Havenith H, Fleurisson J, Grandjean G (2004). Numerical Modelling of Seismic Slope Stability, in Engineering Geology for Infrastructure Planning in Europe, Springer.

Campbell KW (1997). Empirical Near-Source Attenuation Relationships

for Horizontal and Vertical Components of Peak Ground Acceleration, Peak Ground Velocity and Pseudo-Absolute Acceleration Response Spectra, Seismological Res. Lett., 68(1): 154-179.
Cherubini C, Santoro F, Vessia G (2004). Hazard assessment in dynamic slope stability analysis, In Risk Analysis IV, Edited By: C.A. BREBBIA, Wessex Institute of Technology, UK.
Das BM (1993). Principles of Soil Dynamics, HWS Publ., USA.
Erdik M, Alpay BY, Onur T, Sesetyan K, Birgoren G (1999). Assessment of earthquake hazard in Turkey and neighboring regions, Annali di Geofisica, 42: 1125-1138.
Erdik M, Durukal E (2004). Strong Ground Motion, in Recent Advances in Earthquake Geotechnical Engineering and Microzonation, A. Ansal (ed.) , Kluwer Academic Publishers,Netherlans.
ISSMFE (1993). Manual for Zonation on Seismic Geotechnical Hazards, Published By Japanese Society of Soil Mechanics and Foundation Enginering.
JICA-IBB Report (2002). The Study on a Disaster Prevention / Mitigation Basic Plan in Istanbul including Seismic Microzonation in the Republic of Turkey, Final Report, Main Report, December 2002, Pacific Consultants International., OYO Corporation, Japan International Cooperation Agency (JICA), Istanbul Metropolitan Municipality (IMM), p. 729.
Joyner WB, Boore DM (1981). Peak Horizontal Acceleration and Velocity from Strong Motion Records, Including Records from the 1979 Imperial Valley, California, Earthquake, Bull. Seis. Soc. Am., 71(6): 2011-2038.
Nazarian S, Stokoe IKH (1984). In- Situ Shear Wave Velocities from Spectral Analysis of Surface Waves, Proc. 8th Conf. On Earthquake Eng. - S. Francisco, Prentice-Hall, 3: 31-38.
Park CB, Miller RD, Xia J (1999). Multichannel Analysis of Surface Waves (Masw); Geophysics, 64: 800-808.
Park CB, Miller RD, Xia J, Ivanov J (2007). Multichannel analysis of surface waves (MASW)— active and passive methods, THE LEADING EDGE, pp. 60-64.
Stokoe KH, II, Wright GW, James AB, Jose MR (1994). Characterization of geotechnical sites by SASW method, *in*Woods, R. D., Ed., Geophysical characterization of sites: Oxford Pub.
Tamura T (1978). An Analysis of the Relation Ship between the Areal Distribution of Earthquake-Induced Landslides and the Earthquake Magnitude, Geographical Rev. Japan, 51-8: 662-672.